Different Effects of Trifluoroethanol and Glycerol on the Stability of Tropomyosin Helices and the Head-to-Tail Complex

Fernando Corrêa and Chuck S. Farah
Departamento de Bioquímica, Instituto de Química, Universidade de São Paulo, São Paulo, SP, Brazil

ABSTRACT Tropomyosin (Tm) is a dimeric coiled-coil protein, composed of 284 amino acids (410 Å), that forms linear homopolymers through head-to-tail interactions at low ionic strength. The head-to-tail complex involves the overlap of approximately nine N-terminal residues of one molecule with nine C-terminal residues of another Tm molecule. In this study, we investigate the influence of 2,2,2-trifluoroethanol (TFE) and glycerol on the stability of recombinant Tm fragments ($ASTm_{1-142}$, $Tm_{143-284(5OHW269)}$) and of the dimeric head-to-tail complex formed by the association of these two fragments. The C-terminal fragment ($Tm_{143-284(5OHW269)}$) contains a 5-hydroxytryptophan (5OHW) probe at position 269 whose fluorescence is sensitive to the head-to-tail interaction and allows us to accompany titrations of $Tm_{143-284(5OHW269)}$ with $ASTm_{1-142}$ to calculate the dissociation constant (K_d) and the interaction energy at TFE and glycerol concentrations between 0% and 15%. We observe that TFE, but not glycerol, reduces the stability of the head-to-tail complex. Thermal denaturation experiments also showed that the head-to-tail complex increases the overall conformational stability of the Tm fragments. Urea and thermal denaturation assays demonstrated that both TFE and glycerol increase the stability of the isolated N- and C-terminal fragments; however, only TFE caused a significant reduction in the cooperativity of unfolding these fragments. Our results show that these two cosolvents stabilize the structures of individual Tm fragments in different manners and that these differences may be related to their opposing effects on head-to-tail complex formation.

INTRODUCTION

Skeletal muscle tropomyosin (Tm) is a 284-residue α-helical dimeric coiled-coil protein involved in the regulation of muscle contraction through its interactions with troponin and actin (1–5). The coiled-coil motif is a consequence of a heptapeptide repeat (a-b-c-d-e-f-g) in the chemical nature of the residues in the primary structure of the polypeptide chain where hydrophobic residues at positions ''a'' and ''d'' create a dimerization interface that stabilizes the coiled-coil structure. Residues at positions ''e'' and ''g'' are often charged and may form salt bridges with residues ''e′'' and ''g′'' of the other helix (6–10). At low ionic strength, Tm forms long linear polymers in a head-to-tail manner through the overlap of about nine N-terminal residues and nine C-terminal residues from each Tm molecule (6,11). In muscle fibers, this interaction results in the formation of continuous cables of Tm that accompany each strand of the actin filament. These interactions play a role in cooperative processes within and between the repeating structural units of the thin filament, each of which contains seven actins, one Tm, and one troponin complex within a single thin filament strand (2,12,13).

High-resolution structures of the N- and C-termini of Tm have been obtained by NMR and x-ray crystallography (14–17). In the solution structure of a chimeric *N*-acetylated peptide corresponding to residues 1–14 of rabbit Tm followed by 18 residues derived from the coiled-coil region of GCN4, residues 1–29 adopted an α-helical coiled-coil structure with the Tm region less tightly packed than the GCN4 region (14). The crystal structure of a nonacetylated N-terminal fragment (Tm_{1-81}) was also highly α-helical, but in this case the first two residues were observed to adopt an extended conformation as expected due to charge repulsions between α-amino groups (15). In the solution structure of a peptide corresponding to the 34 C-terminal residues ($Tm_{251-284}$) containing a stabilizing mutation N-279K, residues 253–269 adopted a coiled-coil conformation with canonical knobs-into-hole packing. However, interstrand contacts involving residues 270–279 deviated from a coiled-coil structure with the helices oriented in an unusual parallel, linear conformation and residues 280–284 were nonhelical (16). The crystal structure of a chimeric peptide (residues 254–284 of Tm, preceded by 24 residues of GCN4) (17) presented a structure similar to that observed in solution (16). However, residues 267–284 did not exhibit any interhelical contacts within the dimer. Instead, tail-to-tail crystal-packing contacts involving helices from independent dimers were observed (17). At the time of submission of this manuscript we became aware of an online version of a study describing the solution structure of the head-to-tail complex in which the C-terminal domain maintained its splayed conformation (18) observed in the structures of the isolated C-terminal peptides.

The intrinsic conformational flexibility of Tm has been related to its ability to interact with other components of the thin filament and its ability to regulate muscle contraction (15, 19,20). The conformational flexibility observed in the C-terminal structures may be important for binding interactions

Submitted October 2, 2006, and accepted for publication December 21, 2006.

Address reprint requests to Chuck S. Farah, Departamento de Bioquímica, Instituto de Química, Universidade de São Paulo, Av. Prof. Lineu Prestes 748, Cidade Universitária, São Paulo, SP, Brasil 05508-000. Tel.: 55-11-3091-3312 ext. 104; Fax: 55-11-3091-3312 ext. 204.

0006-3495/07/04/2463/13 $2.00

doi: 10.1529/biophysj.106.098541

with the N-terminal of Tm and with troponin (16,17,21). Conditions known or expected to destabilize the helical and coiled-coil structure of the C-terminus (increased negative charge density, low ionic strength) have been shown to stabilize the head-to-tail complex (22–29). These observations suggest that other conditions that stabilize the helical conformation of the Tm C-terminus would also destabilize the formation of the head-to-tail complex. 2,2,2-trifluoroethanol (TFE) has been widely used as an α-helix stabilizing cosolvent (30–38), though no consensus exists regarding the mechanism of stabilization. Some reports have suggested that TFE strengthens intramolecular hydrogen bonding (36), binds directly to proteins (37), or acts as a kosmotrope to increase the free energy of the unfolded state (34,38). Relatively high concentrations of TFE (30% v/v) have been shown to increase the α-helix content in a series of C-terminal Tm fragments and in some cases induced the formation of helical trimers (28). Glycerol is also an agent used to increase the stability of proteins (39–46). It interacts favorably with water but not with nonpolar substances. It is thought that glycerol interacts unfavorably with exposed nonpolar groups on protein surfaces and in this way favors the more compact folded structures in relation to more extended or unfolded conformations (39–41).

In this report, we studied the effect of low concentrations of TFE and glycerol (0%–15% v/v) on the stability of the head-to-tail complex and on the conformational stability of N- and C-terminal fragments of Tm ($ASTm_{1-142}$ and $Tm_{143-284(5OHW269)}$, respectively). $Tm_{143-284(5OHW269)}$ contains a 5-hydroxytryptophan (5OHW) probe at position 269, located 15 residues from the C-terminus of the polypeptide chain. The fluorescence of this tryptophan analog has been shown to be a sensitive probe of the polymerization state of full-length Tm (29,47,48). We observed that both osmolytes increased the stability of Tm fragments. TFE-induced stabilization was greater for the C-terminal fragment than for the N-terminal fragment. TFE also significantly reduced the cooperativity of the urea-induced unfolding of both fragments, whereas cooperativity was essentially unchanged in the presence of glycerol. TFE increased the α-helix content of Tm fragments but induced a decrease in the stability of the head-to-tail complex. Glycerol did not increase α-helix content, and it did not have any apparent effect in the association of the head-to-tail complex. These results suggest that these cosolvents differ in the manner by which they modulate different aspects of Tm secondary, ternary, and quaternary (head-to-tail) structure. The results are consistent with the hypothesis (21,29) that conformational flexibility in N- and C-termini contributes toward the formation of the head-to-tail complex.

MATERIALS AND METHODS

Construction of expression vectors, expression, and purification of Tm fragments

The plasmid vector for the bacterial expression of the $ASTm_{1-142}$ fragment (residues 1–142 of chicken skeletal α-Tm with an Ala-Ser N-terminal fusion) has been described previously (29). The plasmid vector for the expression of the $Tm_{143-284(5OHW269)}$ fragment was constructed by amplifying the sequence corresponding to residues 143–284 using the vector pET-MAS269W (47) as a template. The following oligonucleotides were used in the polymerase chain reaction (PCR): *Nde*M142 (5′-GAA GAG AAG CAT ATG ATC CAA GAG ATC-3′) and *Eco*RI(-) (5′-CAT TAA CCT ATA AAA ATA GGC G-3′). The PCR product was digested with *Nde*I and *Eco*RI and subsequently ligated into vector pET3a (49) previously digested with the same restriction enzymes. The $ASTm_{1-142}$ fragment was expressed and purified as described (29,50). The fragment $Tm_{143-284(5OHW269)}$ containing a 5OHW probe at position 269 was expressed and purified as described (47,51). Protein concentrations were determined by the modified Lowry method (52).

Fluorescence titration experiments and calculation of head-to-tail complex dissociation constant

Titration experiments were performed using an AVIV (Lakewood, NJ) ATF105 automated titration differential/ratio spectrofluorimeter. The emission spectra were collected between 338–342 nm (bandwidth: 5–7 nm) using an excitation wavelength of 295 nm and bandwidths of 0.5–1 nm. Proteins were dissolved in 54.5 mM MOPS (3-(*N*-morpholino)propanesulfonic acid) pH 7.0, 0.5 mM EDTA, 1 mM 1,4-dithiothreitol (DTT), 0%–20% (v/v) TFE or 15% glycerol at 25°C. Each titration experiment began with an initial concentration of 2 μM (dimer) $Tm_{143-284(5OHW269)}$. Fluorescence emission spectra were collected after the addition of aliquots of $ASTm_{1-142}$ in 0.2-μM (dimer) increments. The samples were equilibrated for 3 min before each measurement.

To calculate the dissociation constant for the head to tail complex, consider the following dimerization reaction:

$$N + C \leftrightarrow NC,$$

where N is a free N-terminal coiled-coil dimer ($ASTm_{1-142}$), C is a free C-terminal coiled-coil dimer ($Tm_{143-284(5OHW269)}$), and NC is a head-to-tail complex. It can be shown that

$$[NC]^2 - [NC]([N]_{total} + [C]_{total} + K_d) + [N]_{total}[C]_{total} = 0.$$
$$\text{Where} \quad K_d = [N][C]/[NC], \quad [N]_{total} = [N] + [NC]$$
$$\text{and} \quad [C]_{total} = [C] + [NC]. \tag{1}$$

The 5OHW probe in $Tm_{143-284(5OHW269)}$ can exist in two environments: free (C) or in the complex (NC), with different fluorescence emission intensity in each state (F_o and F_{max}, respectively) (47). The concentration of the head-to-tail complex [NC] at each point in the titration is

$$[NC] = \{(F - F_o(v/V))/((F_{max} - F_o)(v/V))\}[C]_{total}, \tag{2}$$

where F_o is the initial fluorescence intensity in the absence of N-terminal, F is the fluorescence at any given point in the titration, v is the initial volume, and V is volume at any given point in the titration. We can consider the maximum relative fluorescence change as

$$\alpha = F_{max}/F_o. \tag{3}$$

Combining Eqs. 1, 2, and 3, we are able to express F in terms of $[N]_{total}$, $[C]_{total}$, K_d, and α,

$$F = (v/V)((\alpha - 1)/(2[C]_{total})([N]_{total} + [C]_{total} + K_d - ((([N]_{total} + [C]_{total} + K_d)^2) - 4[N]_{total}[C]_{total})^{1/2}) + 1) \tag{4}$$

Nonlinear regression fitting of fluorescence titration curves to Eq. 4 using SigmaPlot (SPSS, Chicago, IL) allows for the estimation of parameters K_d and α. In all cases the value of α was set to 1.23.

Circular dichroism spectroscopy

Proteins (10 μM dimer) were dissolved in 54.5 mM MOPS, pH 7.0, 0.5 mM EDTA, 1 mM DTT, 0%–15% TFE or glycerol. Far-ultraviolet (UV) circular dichroism (CD) spectra (200–260 nm) were collected in a Jasco-720 spectropolarimeter (Jasco, Tokyo, Japan) at 20°C, 100 nm/min, and a response time of 4 s, using a 0.5-mm cuvette. The spectra shown are the average of four individual scans.

Urea and thermal denaturation monitored by circular dichroism

Urea denaturation assays were performed in 54.5 mM MOPS, pH 7.0, 0.5 mM EDTA, 1 mM DTT, 0%–15% TFE or glycerol. A stock of 9 M urea solution (Sigma, St. Louis, MO; ultrapure grade) was prepared in the above buffer and mixed with individual protein samples to achieve the desired final concentration of urea and protein (10 μM dimer). The urea concentration was confirmed by refractive index measurements (53). Samples were equilibrated at 20°C for 1 h before recording the CD spectra. The urea denaturation curve was analyzed using Eq. 7 derived from the thermodynamic parameters (Eqs. 5 and 6) for dimeric proteins proposed by Mateu and Fersht (54):

$$\Delta G_u = -RT\ln\{[2P_t(Y-(Y_f+m_f[D]))^2]/[(Y_u+m_u[D]-Y)(Y_u-Y_f+[D](m_u-m_f))]\} \quad (5)$$

$$\Delta G_u = m([D]_{1/2}-[D]) - RT\ln P_t \quad (6)$$

$$Y = (2\exp(m([D]_{1/2}-[D])/RT)(Y_f+m_f[D]) - (Y_u+m_u[D]) + (Y_f+m_f[D]) + (\exp(m([D]_{1/2}-[D])/RT)((2(Y_f+m_f[D]-Y_u-m_u[D]))^2) + ((Y_f+m_f[D]-Y_u-m_u[D])^2))^{1/2})/(2\exp(m([D]_{1/2}-[D])/RT)), \quad (7)$$

where Y is the mean residual ellipticity at 222 nm, Y_f and Y_u are intercepts that define the pretransition and posttransition baselines, respectively, m_f and m_u are the steepness of the pre- and posttransition baselines, respectively, m is the steepness of the transition region, $[D]$ is the urea concentration, $[D]_{1/2}$ is the urea concentration at which 50% of the molecules are unfolded (assuming a two-state transition), and P_t is the protein concentration. Thermal denaturations were performed in the above buffer in the presence of 0%, 7.5%, and 15% (v/v) TFE or glycerol. The measurements at 222 nm were collected at 2°C intervals from 4°C to 80°C and back to 4°C at a velocity of 1°C/min.

Gluteraldehyde cross-linking experiments

Proteins were equilibrated for 30 min under the conditions described in the figure legend. Gluteraldehyde was added to a final concentration of 0.005%, and after 10 min the cross-linking reaction was stopped by the addition of sodium dodecyl sulfate (SDS)-PAGE sample buffer (0.1 M Tris-HCl (pH 6.8), 3.7% SDS, 18.7% glycerol, 1.35 mM β-mercaptoethanol, 0.01% bromophenol blue). The products of the cross-linking reaction were analyzed by 15% SDS-PAGE.

RESULTS AND DISCUSSION

TFE increases the helical content of Tm fragments

To evaluate the effect of TFE and glycerol on the secondary structure of the Tm fragments we collected CD spectra in MOPS buffer containing 0%, 7.5%, and 15% TFE or glycerol (Fig. 1). The presence of TFE promoted an increase in the α-helix content of the Tm fragments as indicated by a significant increase in the magnitude of the negative ellipticity at 222 nm (Fig. 1). The TFE-induced increase of the α-helical content in the two Tm fragments is consistent with its previously demonstrated capacity to stabilize the helical conformation in helix-forming polypeptides (30–38). However the addition of up to 15% glycerol did not affect the CD spectra of the two fragments (Fig. 1). In a previous study, no glycerol-induced increment in α-helical content was observed for an engineered dimeric leucine zipper (41). The $\Theta_{222}/\Theta_{208}$ ratio, which has been associated with the coiled-coil conformation of proteins (55–58), did not change significantly in the presence of TFE (data not shown).

TFE and glycerol stabilize the Tm coiled-coil

To investigate the relationship between the stability of the Tm coiled-coil and the stability of the head-to-tail complex, we began by measuring the effect of low concentrations of TFE and glycerol on the stability of the Tm fragments. We performed urea denaturations of both fragments at different cosolvent concentrations (0%, 5%, 10%, 15%). Fig. 2 presents the residual ellipticity at 222 nm of the proteins as a function of urea concentration. Inspection of the denaturation curves shows that TFE and glycerol significantly increased the stability of both Tm fragments. Significant increases in stability were observed even at low cosolvent concentrations (5%). Table 1 lists the urea concentration at the centers of the unfolding transitions ($[\text{urea}]_{1/2}$) and the apparent cooperativity of the transitions reflected by the parameter m. The stability of both fragments increased with increasing concentrations of cosolvent. However the stabilizing effect of TFE was more pronounced than that of glycerol. We also performed thermal denaturations of the Tm fragments in the presence of 0%, 7.5%, and 15% TFE or glycerol (Fig. 3). The thermal stabilities of both fragments increased in the presence of cosolvents (Fig. 3, Table. 2). Comparing values obtained with 0% and 15% TFE, the thermal stability of the C-terminal fragment presented a more expressive change

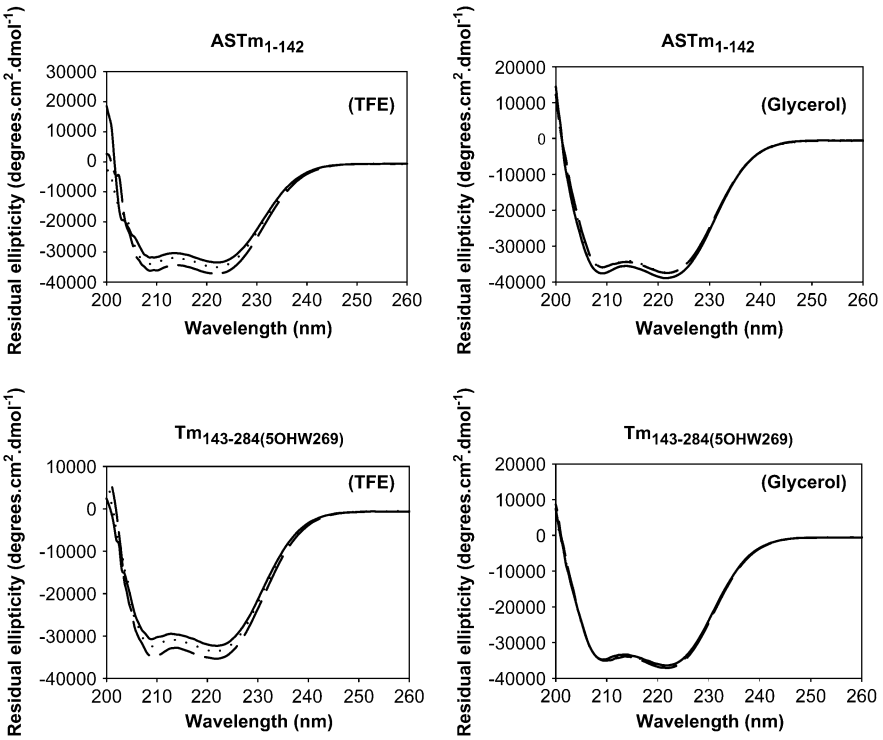

FIGURE 1 Far-UV CD spectra of $ASTm_{1–142}$ and $Tm_{143–284(5OHW269)}$ at various concentrations of TFE. The analyzed fragment is indicated above each panel. Conditions: 54.5 mM MOPS, pH 7.0, 0.5 mM EDTA, 1 mM DTT at 25°C. Solid line, 0% TFE/glycerol; dotted line, 7.5% TFE/glycerol; broken line, 15% TFE/glycerol.

(transition midpoint temperature (T_m) increasing from 33.7°C to 46.8°C), when compared to the N-terminal fragment (40.2°C–46.3°C). It is interesting to observe that in the absence of TFE the N-terminal fragment is much more stable than the C-terminal fragment, whereas in the presence of 15% TFE, the two fragments display very similar transition midpoint temperatures (Table 2). Glycerol significantly raised the thermal stability of both the N-terminal fragment (40.2°C–49.9°) and the C-terminal fragment (33.7°C–44.2°C) (Fig. 3 and Table 2).

The Tm coiled-coil is maintained in 15% TFE and in 15% glycerol

One can imagine two possible ways in which the urea-induced denaturation of Tm coiled-coils could proceed: i) a

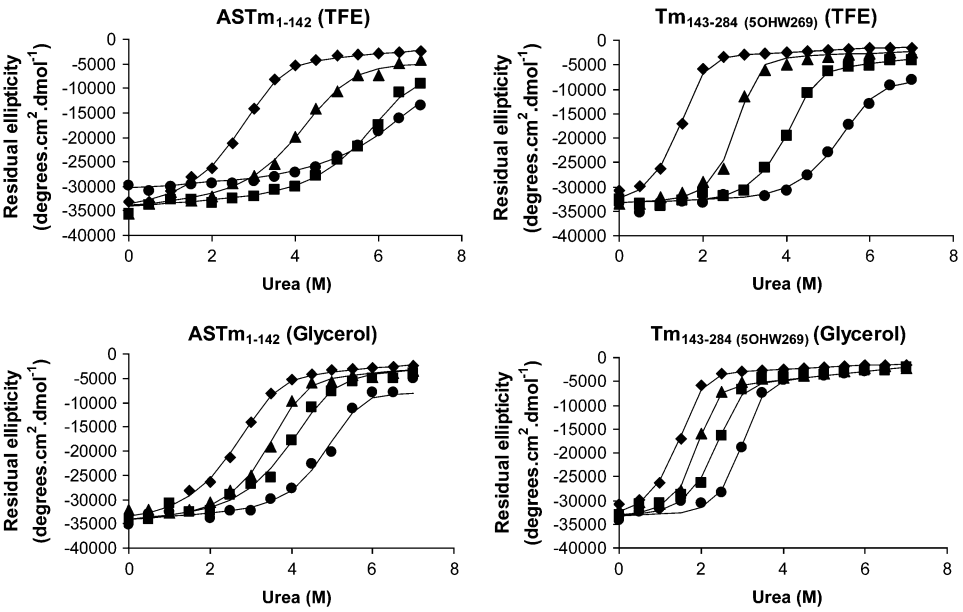

FIGURE 2 Urea denaturation of $ASTm_{1–142}$ and $Tm_{143–284(5OHW269)}$. Residual ellipticity at 222 nm is shown as a function of urea concentration in the presence of (♦) 0% TFE/glycerol; (▲) 5% TFE/glycerol; (■) 10% TFE/glycerol; (●) 15% TFE/glycerol. Condition: 54.5 mM MOPS pH 7.0, 0.5 mM EDTA, 1 mM DTT at 25°C. Protein concentration: 10 μM (dimer). The lines correspond to the least squares fitted curves (see Materials and Methods).

TABLE 1 Urea denaturation parameters for the Tm fragments as a function of TFE and glycerol concentration

	$[urea]_{1/2}$ (M)	m (Kcal mol^{-1} M^{-1})
$ASTm_{1-142}$	2.88	1.54
$ASTm_{1-142}$ 5% TFE	4.43	1.33
$ASTm_{1-142}$ 5% Glycerol	3.65	1.85
$ASTm_{1-142}$ 10% TFE	6.04	1.38
$ASTm_{1-142}$ 10% Glycerol	4.22	1.50
$ASTm_{1-142}$ 15% TFE	6.73	1.13
$ASTm_{1-142}$ 15% Glycerol	5.08	1.86
$Tm_{143-284\ (5OHW269)}$	1.57	2.59
$Tm_{143-284\ (5OHW269)}$ 5% TFE	2.91	2.98
$Tm_{143-284\ (5OHW269)}$ 5% Glycerol	1.98	3.18
$Tm_{143-284\ (5OHW269)}$ 10% TFE	4.16	2.29
$Tm_{143-284\ (5OHW269)}$ 10% Glycerol	2.48	2.55
$Tm_{143-284\ (5OHW269)}$ 15% TFE	5.50	1.72
$Tm_{143-284\ (5OHW269)}$ 15% Glycerol	3.10	3.03

single step process in which the breaking of interhelical contacts is simultaneously accompanied by helical denaturation, or ii) a two-step process in which helices separate but remain intact at a low concentration of urea and only denature at higher urea concentrations. In aqueous solutions, the first scenario is much more likely since, as has been pointed out previously (28,59), the Tm sequence has an intrinsically low helix-forming propensity and the helical state is most likely stabilized by interhelical contacts within the coiled-coil structure. However, high concentrations of TFE have been shown to increase and stabilize the α-helical content of proteins while at the same time disrupting tertiary interactions (60–62). To evaluate the impact of low TFE concentration (15%) in the coiled-coil structure, we performed thermal denaturations varying the protein concentration in the absence and presence of 15% TFE (Fig. 4). The stability of oligomeric proteins is concentration dependent; in thermal denaturations, the T_m shifts to higher values as the protein concentration is increased (63–65). If TFE stabilizes the Tm α-helix while at the same time destabilizing the coiled-coil, the T_m would be expected to increase at higher protein concentrations in the absence of TFE and not increase (or at least increase less) in the presence of TFE. Our results show that increments in protein concentration increased the T_m both in the absence and presence of 15% TFE (Fig. 4). The increase in T_m observed upon increasing the total monomer concentration from 2 μM to 30 μM was similar for both N- and C-terminal Tm fragments: the T_m of the N-terminal fragment increased 3.6°C (from 38.6°C to 42.2°C) in the absence and 4.5°C (from 44.8°C to 49.3°C) in the presence of TFE, whereas the variation observed for the C-terminal fragment was 2.8°C (from 32.0°C to 34.8°C) in the absence and 3.8°C (from 44.7°C to 48.5°C) in the presence of TFE (Fig. 4). These results indicate that stabilization of the Tm helix by TFE does not seem to be accompanied by any significant change in the monomer-dimer equilibrium of the Tm coiled-coil.

Using a different approach, we obtained a direct measure of the extent of coiled-coil formation during the urea denaturations by carrying out glutaraldehyde cross-linking experiments on samples containing varying amounts of urea (0, 4, and 6.5 M) and/or TFE or glycerol (0% and 15%). In these experiments, coiled-coils can be detected by the appearance of a band in SDS-PAGE that migrates at double the molecular weight of the single polypeptide chain. In the absence of TFE, glycerol and urea, an amount of dimer could be detected for both fragments but to a lesser extent for the C-terminal fragment (Fig. 5, lanes 1 and 7). The addition of 4 M or 6.5 M urea completely abolished dimer formation (Fig. 5, lanes 2, 3, 8, 9). This is consistent with the urea denaturation curves in which both fragments are completely unfolded at 4 M urea (Fig. 2 and Table 1). Furthermore, the presence of 15% TFE stabilized the coiled-coil state of $ASTm_{1-142}$ to such an extent that an amount of dimer could be detected even in the presence of 6.5 M urea (Fig. 5 *top*, lane 6). On the other hand, very little $Tm_{143-284(5OHW269)}$ dimer could be detected in 15% TFE + 6.5 M urea (Fig. 5 *top*, lane 12), whereas it could be detected in the presence of 15% TFE + 4 M urea (Fig. 5 *top*, lane 11). These observations are consistent with the urea denaturation profiles of these fragments in which the N-terminal fragment has a $[urea]_{1/2}$ of 6.73 M and is therefore not completely denatured at 6.5 M urea, whereas the C-terminal fragment ($[urea]_{1/2}$ = 5.50 M) is folded at 4 M urea but denatured at 6.5 M urea (Fig. 2 and Table 1). The addition of glycerol stabilized the Tm fragments (Fig. 5 *bottom*): we could detect dimers in 4 M urea for the N-terminal (lane 5) but not for the C-terminal (lane 11). The results obtained are consistent with a model in which the breaking of interhelical contacts and helical denaturation are simultaneous and highly coupled. TFE has been shown to induce the formation of higher molecular weight aggregates in many proteins (66–68), and 30% TFE induces the formation of trimers in certain C-terminal Tm fragments (28). However, we did not observe TFE-induced trimer formation in glutaraldehyde cross-linking experiments in this study, possibly because these experiments were performed at lower TFE concentrations (0%–15%).

Differences in the cooperativities of Tm coiled-coil denaturations in the presence of TFE and glycerol

TFE induced a significant reduction in the cooperativity parameter (m) of urea denaturations of both Tm fragments, whereas this parameter varied very little upon addition of glycerol (Table 1). Similar effects were observed in the thermal denaturation experiments of the individual fragments: in the presence of TFE unfolding was less cooperative (compare *curves* in Fig. 3, *A* and *C*) whereas glycerol did not affect the slope of unfolding transition (compare *curves* in Fig. 3, *A* and *E*).

The m-value is defined as the rate of change in free energy as a function of denaturant concentration and it is considered to be proportional to the amount of buried protein surface

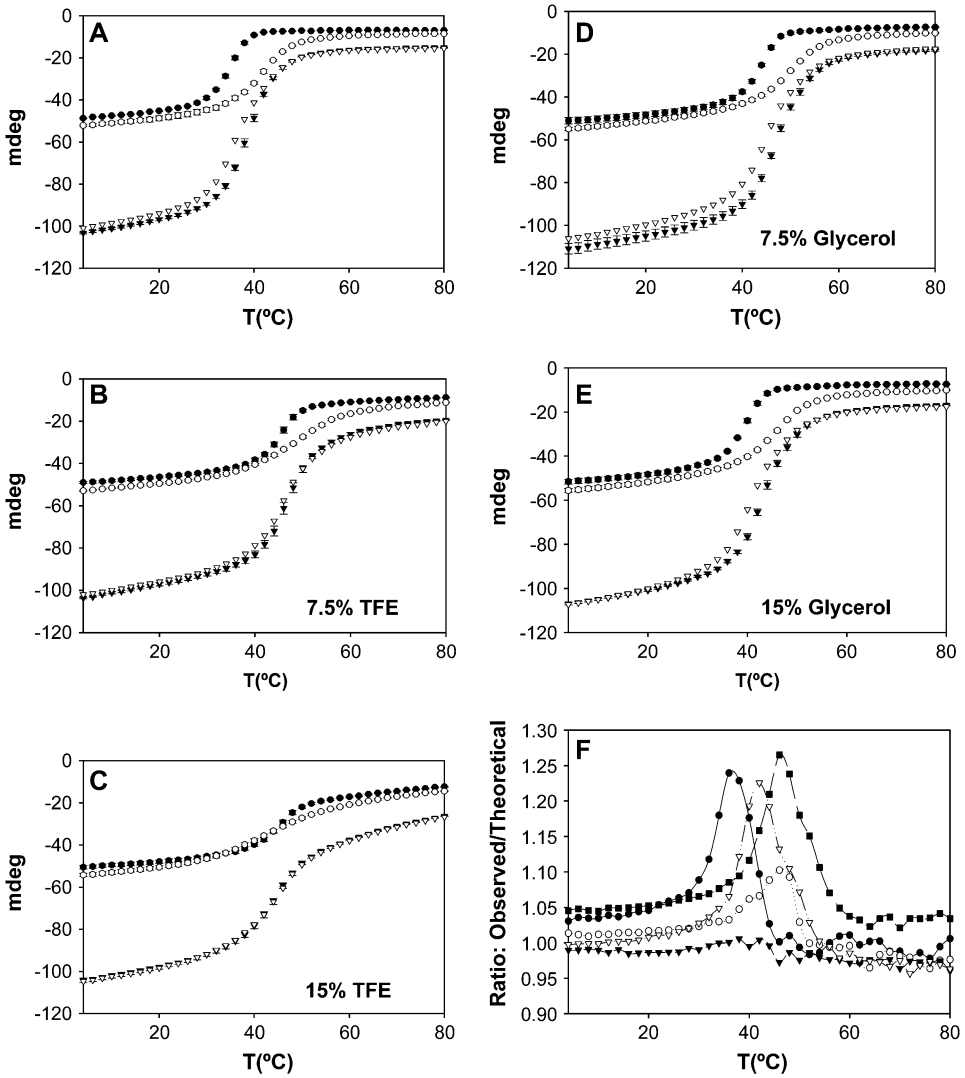

FIGURE 3 Thermal denaturation curves of $ASTm_{1–142}$, $Tm_{143–284(5OHW269)}$, and 1:1 mixtures. (*A*, *B*, *C*, *D*, and *E*) Ellipticities (222 nm) as a function of temperature (4°C–80°C) measured at three TFE/glycerol concentrations: no cosolvent (*A*), 7.5% TFE (*B*), 15% TFE (*C*), 7.5% glycerol (*D*), 15% glycerol (*E*). Conditions: 54.5 mM MOPS pH 7.0, 0.5 mM EDTA, 1 mM DTT. Protein concentration: 10 μM (dimer). (○) $ASTm_{1–142}$; (●) $Tm_{143–284(5OHW269)}$; (▲) 1:1 mixture of $ASTm_{1–142}$ and $Tm_{143–284(5OHW269)}$ (observed); (Δ) Sum of the individual $ASTm_{1–142}$ and $Tm_{143–284(5OHW269)}$ curves (theoretical). Each point is the average (± SD) of three experiments. (*F*) Ratio between experimental and theoretical thermal denaturation curves (observed/theoretical negative ellipticities) observed at the different cosolvent concentrations. (●) no cosolvent; (○) 7.5% TFE; (▲) 15% TFE; (Δ) 7.5% glycerol; (■) 15% glycerol.

exposed to solvent when the protein unfolds (69–71). Myers et al. (70) found a correlation between *m*-values with the change in calculated solvent accessible surface area (ΔASA) upon unfolding for 45 proteins: proteins with a greater ΔASA had a higher *m*-value than proteins with a lower ΔASA. Pace et al. (69) observed that urea denaturation of ribonuclease A and T1 was more cooperative at pH values in which the absolute value of the liquid charge of the protein was large and interpreted this as resulting from an increased solvent-accessible surface area in the unfolded native state which comes about from repulsive interactions between like charges. Shortle (71) observed dramatically different effects of single mutations on the amount of residual structure within the denatured state (as reflected by *m*-values) of staphylococcal nuclease and concluded that mutations may shift the distribution among subsets of denatured microstates with significantly different ASAs.

TABLE 2 Thermal denaturation transition midpoint temperatures (°C) of Tm fragments as a function of TFE and glycerol concentration

[cosolvent] (v/v)	$ASTm_{1–142}$	$Tm_{143–284(5OHW269)}$
No cosolvent	40.2	33.7
7.5% TFE	47.9	44.5
7.5% Glycerol	45.6	40.1
15% TFE	46.3	46.8
15% Glycerol	49.9	44.2

The differences in the cooperativities of unfolding observed in glycerol/water and TFE/water mixtures are not completely unexpected since these two cosolvents act upon the stability of the coiled-coil dimers by different mechanisms. Kentsis and Sosnick (34) suggested that TFE-induced helix formation in the coiled-coil portion of GCN4 is due to a reduction in the hydrogen-bonding capacity of water, which in turn stabilizes intramolecular hydrogen bonds in relation to intermolecular (protein-water) hydrogen bonds; in essence, TFE destabilizes the unfolded state (34,72,73) On the

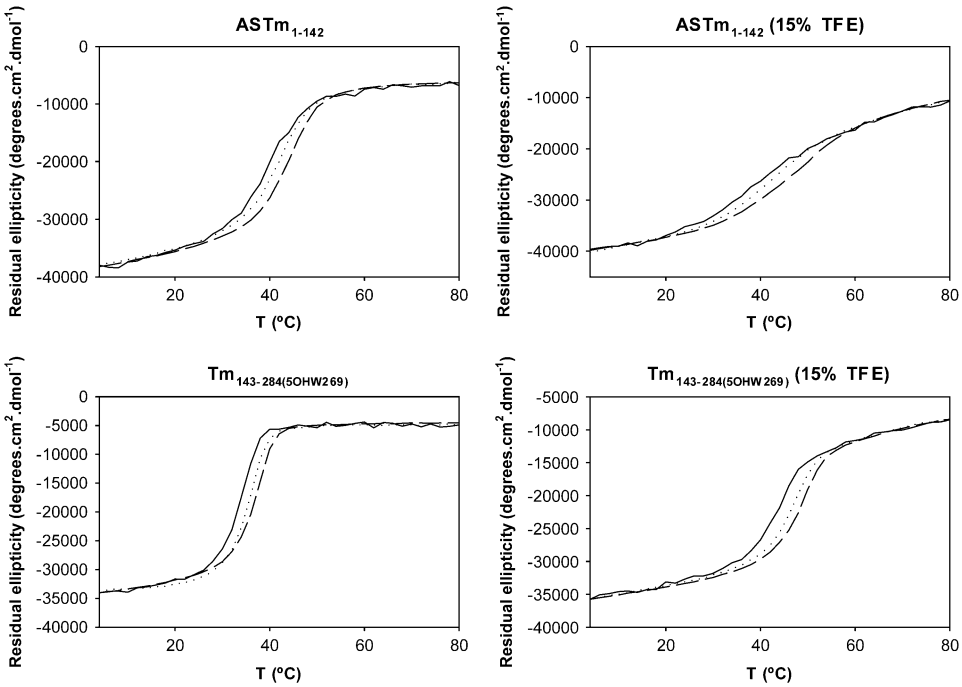

FIGURE 4 Concentration dependence of thermal denaturation of $ASTm_{1–142}$ and $Tm_{143–284(5OHW269)}$ in the absence and presence of 15% TFE. Ellipticities (222 nm) as a function of temperature (4°C–80°C) measured at three protein concentrations (dimer). Solid line, 2 μM protein; dotted line, 10 μM protein; and broken line, 30 μM protein. Conditions: 54.5 mM MOPS, pH 7.0, 0.5 mM EDTA, 1 mM DTT, ±15% TFE (v/v).

other hand, the mechanism of stabilization proposed for glycerol is based on the preferential exclusion of the cosolvent from the protein domain, which stabilizes the more compact native structure in which the solvent-accessible area has been minimized (39–41,74). Dürr and Jelesarov (41) studied the stabilizing effect of glycerol on an engineered coiled-coil protein and observed a glycerol-induced reduction in heat capacity of unfolding (ΔC_p^{unf}). Since a positive ΔC_p^{unf} heat capacity is related to the exposure of nonpolar surfaces upon unfolding, a reduction in ΔC_p^{unf} is consistent with either a less compact folded state or a more compact unfolded state (41). The latter hypothesis is more likely since glycerol would not be expected to alter the structure (no observed change in Θ_{222}, see above) or solvent accessibility of the folded state (41).

Based on the above observations, we can attempt to rationalize the different effects of TFE and glycerol on Tm coiled-coil helical content, stability, and *m*-value behavior (cooperativity). Glycerol did not increase the α-helix content of the Tm fragments and probably increases Tm stability by favoring the packing of already folded coiled-coil regions without inducing α-helix formation. This is consistent with the small changes in *m*-value observed in the presence of glycerol. TFE not only increased Tm coiled-coil stability, but also increased the α-helix content in both N- and C-terminal fragments, which suggests that the folded state has been altered to one with a possibly reduced solvent accessible surface area. A good candidate region for this structural alteration in $Tm_{143–284(5OHW269)}$ is the extreme C-terminus whose structure was found to be more open in both solution and crystal structures (16,17). The fact that the heptapeptide repeat is sustained all along this region (6) is consistent with this hypothesis. However, TFE decreases the *m*-value of Tm denaturation, suggesting that the unfolded state in TFE is also less solvent-exposed than in water or in glycerol, possibly due to cosolvent-induced desolvation, which favors the formation of intramolecular hydrogen bonds as has been suggested in other studies (34).

TFE, but not glycerol, destabilizes the head-to-tail complex

We have previously shown that the fluorescence of a 5OHW at position 269, located 15 residues from the C-terminus is a sensitive probe of the polymerization state of full-length ASTm (29,47). We used this probe to study the effect of TFE and glycerol on the strength of the head-to-tail interaction between isolated Tm fragments ($ASTm_{1–142}$ and $Tm_{143–284(5OHW269)}$). The use of fragments allows us to reduce the complex polymerization process (47) into one of simple dimerization and allowed us to measure the energy of association involved in the formation of the head-to-tail complex as a function of TFE and glycerol concentrations.

Fluorescence measurements of $Tm_{143–284(5OHW269)}$ during titrations with $ASTm_{1–142}$ in the presence of 0%–15% TFE are shown in Fig. 6 *A*. The titration curves could be used to calculate the dissociation constant and the free energy of association involved in the formation of the head-to-tail complex as described in Materials and Methods. Titrations performed in the presence of TFE at concentrations >15% did not produce significant changes in $Tm_{143–284(5OHW269)}$ fluorescence. Fig. 6 *B* presents the free energy of association and

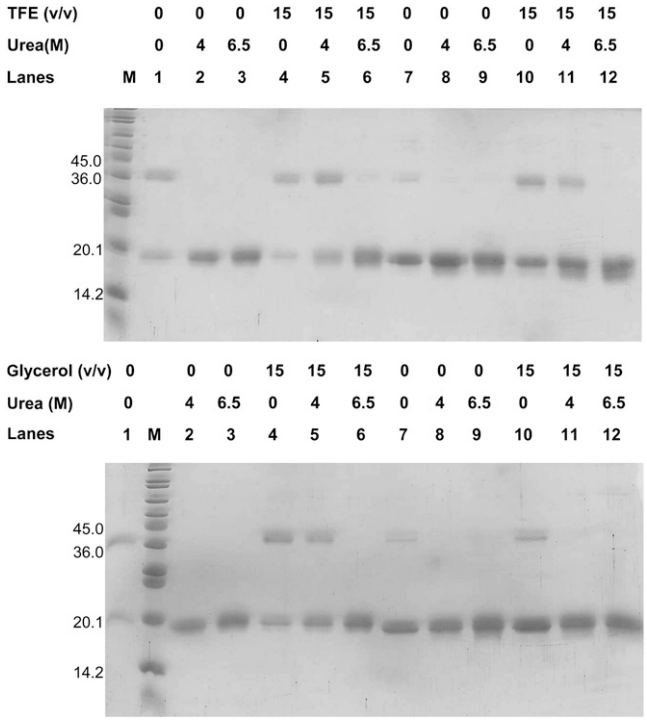

FIGURE 5 Glutaraldehyde cross-linking of Tm fragments. Proteins were equilibrated for 1 h at 25°C in the presence of varying concentrations of TFE and urea as indicated in the figure followed by treatment with 0.005% glutaraldehyde for 10 min. M: Molecular mass marker (6,500–205,000 Da); lane 1: $ASTm_{1-142}$; lane 2: $ASTm_{1-142}$ + 4 M urea; lane 3: $ASTm_{1-142}$ + 6.5 M urea; lane 4: $ASTm_{1-142}$ + 15% cosolvent (v/v); lane 5: $ASTm_{1-142}$ + 4 M urea + 15% cosolvent (v/v); lane 6: $ASTm_{1-142}$ + 6.5 M urea + 15% cosolvent (v/v); lane 7: $Tm_{143-284(5OHW269)}$; lane 8: $Tm_{143-284(5OHW269)}$ + 4 M urea; lane 9: $Tm_{143-284(5OHW269)}$ + 6.5 M urea; lane 10: $Tm_{143-284(5OHW269)}$ + 15% cosolvent (v/v); lane 11: $Tm_{143-284(5OHW269)}$ + 4 M urea + 15% cosolvent (v/v); lane 12: $Tm_{143-284(5OHW269)}$ + 6.5 M urea + 15% cosolvent (v/v). Conditions: 54.5 mM MOPS, pH 7.0, 0.5 mM EDTA, 1 mM DTT at 25°C. Protein concentration: 2 μM (dimer).

calculated dissociation constants (K_d) as a function of TFE concentration. The results indicate a decrease in the stability of the head-to-tail complex with increasing TFE concentration. The addition of 15% TFE results in an ~10-fold change increase in K_d. These results show that the TFE-induced structural changes and the increased conformational stability of the Tm fragments reduced the stability of the head-to-tail complex. Glycerol, on the other hand, did not appreciably affect the stability of the head-to-tail complex as can be observed by comparing the titration curves obtained for the presence and absence of 15% glycerol (Fig. 6 *C*). This observation indicates that the nature of the conformational stabilization by glycerol manifests itself differently from that of TFE in terms of the head-to-tail complex.

The destabilizing effect of TFE on the head-to-tail complex could also be observed, although indirectly, by comparing the observed thermal denaturation profiles of mixtures of $ASTm_{1-142}$ and $Tm_{143-285(5OHW269)}$ at varying TFE concentrations with the ''theoretical'' profiles calculated from the sum of the denaturation profiles of the isolated fragments (Fig. 3). Comparison of the thermal denaturation profiles in the transition regions of the experimentally observed and theoretical curves reveals small but significant differences in the absence of TFE (Fig. 3 *A*). The addition of 7.5% TFE greatly reduced this difference (Fig. 3 *B*), and 15% TFE abolished it altogether (Fig. 3 *C*). Fig. 3 *F* shows the ratio between experimental and theoretical thermal denaturation curves (observed/theoretical negative ellipticities as a function of temperature) observed at the different cosolvent concentrations. This figure shows that at the midpoint of the transition in the absence of cosolvents, the experimentally observed negative ellipticity was 24% greater than that of the theoretical curve (Fig. 3 *F*). In the presence of 7.5% TFE the shift was only 7%, and at 15% TFE no significant shift was observed (Fig. 3 *F*). These results are consistent with the hypothesis that i) in the absence of TFE the formation of the head-to-tail complex stabilizes the helical conformation of the polypeptide chains, and ii) the stabilizing and folding effects of TFE on the chain conformation is related to a destabilization of the head-to-tail complex. The same analysis was performed in the presence of glycerol. This cosolvent increased the stability of the Tm fragments but did not significantly change the shift between observed and theoretical curves (Fig. 3, *D* and *E*). Fig. 3 *F* shows that in the presence of glycerol the ratio between observed and theoretical ellipticities at the midpoint at the transition was maintained at 1.25. We have previously obtained similar results using smaller and truncated C-terminal Tm fragments in the absence of cosolvents (29). In that study, the incremental stability shift due to head-to-tail complex formation was greater since the C-terminal fragments employed were inherently less stable than $Tm_{143-284(5OHW269)}$. This also explains why no significant differences between the theoretical and observed curves were observed in the pretransition regions in this study.

Tm function, flexibility, and head-to-tail complex formation

In the muscle thin filament, Tm interacts with itself as well as with actin and troponin. Several modifications of the N- and C-termini of Tm affect its ability to polymerize and reduce its affinity for actin (50,75–77). Troponin increases Tm viscosity, promotes the polymerization of nonpolymerizable Tms (50,78), and restores the ability of nonpolymerizable Tms to interact with actin (50,79–85). However, the role of the head-to-tail interaction on the cooperativity of Tm binding to actin is not clear. Troponin and S1-induced binding of Tm to actin indicates that Tm polymerization contributes more toward the intrinsic affinity of Tm for actin than to the cooperativity of binding to actin (81–87). For example, Moraczewska et al. (86) showed that several nonpolymerizable Tm mutants (lacking the nine amino acids at one or both termini) can be induced to bind cooperatively to actin by myosin subfragment S1.

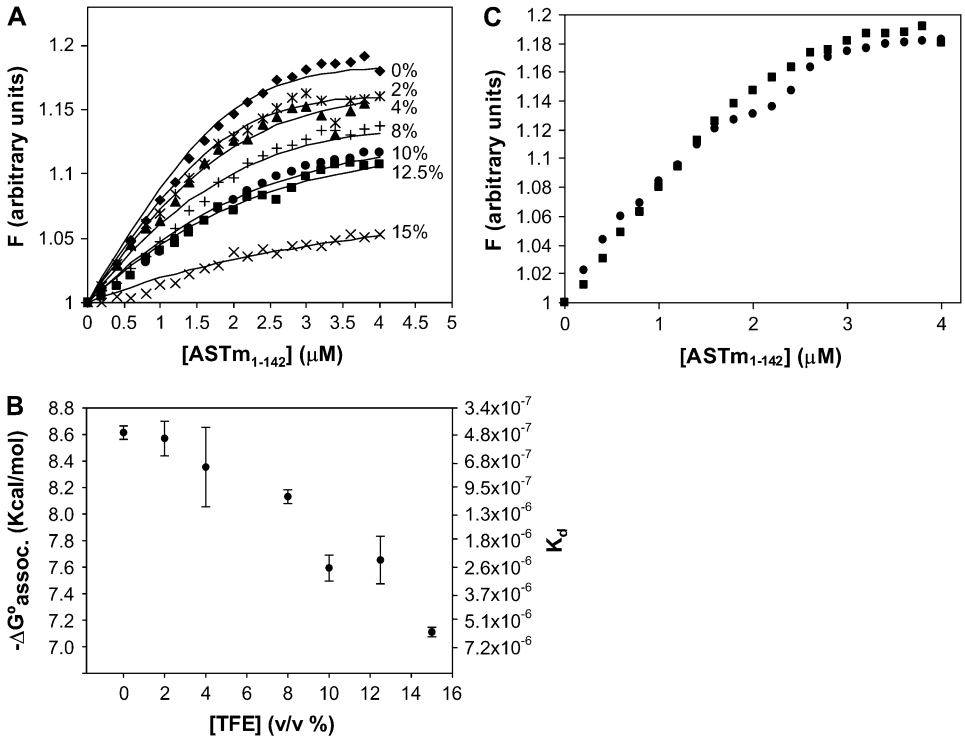

FIGURE 6 Head-to-tail complex formation. (*A*) The fluorescence of $Tm_{143–284(5OHW269)}$ was monitored during its titration with $ASTm_{1–142}$ in the presence of several TFE concentrations (v/v). The TFE concentrations are indicated in the panel. Conditions: 54.5 mM MOPS (pH 7.0), 0.5 mM EDTA, 1 mM DTT at 25°C. All the samples were preequilibrated for 3 min before determining the fluorescence measurements. The lines indicate the calculated least squares fitted curves for the data (see Material and Methods). (*B*) Free energy of association ($\Delta G°_{assoc}$) and K_d values for the $ASTm_{1–142}$-$Tm_{143–284(5OHW269)}$ complex as a function of TFE concentration. Free energy values were determined from the dissociation constants calculated from the least squares fitted curves in *A*. Each point is the average (± SD) of at least three experiments. (*C*) Comparison between the titration curve in the absence of cosolvent (■) and the titration curve in the presence of 15% glycerol (●).

There is evidence that the conformational flexibility of the Tm molecule is important for its ability to interact with other muscle proteins and carry out specific functions. For example, Tm polymers must follow helical tracks along and around the actin filament and Tm's intrinsic instability may permit it to adopt multiple conformational states that can be associated with distinct functional states of the thin filament: the ''blocked'', ''off'', and ''on'' states (3,7,15,88–91). The crystal structure of an 81-residue N-terminal Tm fragment revealed that regions rich in alanine residues at ''a'' and ''d'' positions of the coiled-coil repeat corresponded to bends in the Tm supercoil caused by local breaks in the twofold symmetry of the coiled-coil and staggering of the polypeptide chains (15). Mutation of some of these alanine residues to residues more often found in canonical coiled-coils increased Tm stability while at the same time reducing its affinity for actin (92,93).

Denaturation studies have shown that the C-terminal half of Tm is less stable than the N-terminal half (94,95) (Tables 1 and 2). High-resolution structural data of the Tm C-terminal region have revealed a noncanonical coiled-coil conformation with significant structural flexibility in which the coiled-coil structure gradually comes apart over the last 15 residues (16,17); this, despite the fact that the heptad repeat is maintained in this region. The highly conserved nature of the heptad repeat right up to residue 284 argues that the C-terminus could adopt a coiled-coil structure in vivo in the context of the thin filament. However, the recent structure resolved by NMR to the head-to-tail complex between peptide models ($Tm_{1–14}$ and $Tm_{251–284}$) of rat α-Tm demonstrated that the splayed conformation of the C-terminal region is maintained in the head-to-tail complex (18). The splaying of chains in the Tm C-terminal creates a cleft that allows interfacial interactions with 11 residues from the N-terminal chains. In this highly symmetrical structure, the plane of the N-terminal coiled-coil is rotated 90° relative to the plane parallel to the C-terminal chains.

Greenfield et al. (21) have demonstrated that a Q263L mutation increased the stability of a small C-terminal fragment ($Tm_{251–284}$) while at the same time reducing its affinity for a Tm N-terminal fragment and for troponin. Paulucci et al. (29) demonstrated that a Tm fragment ($ASTm_{1–260}$) containing a greater concentration of negative charges at its C-terminus is conformationally less stable but polymerizes to a greater extent than full-length ASTm. It was proposed that the greater concentration of negative charges at the nonnative C-terminus destabilized the individual α-helices as well as interhelical contacts, favoring a more extended nonhelical conformation (29). Interestingly, the destabilization of the Tm N-terminus has an opposite effect: the presence of a charged α-amino group at an ''a'' position in nonacetylated Tm destabilizes the structure of the N-terminus (14,15) and reduces the head-to-tail association (50,86). An Ala-Ser extension (50) or a five amino acid extension (Tm-exon 1b) (86) restores complex formation due to the dislocation of the charged α-amino group to an external position (not ''a'' or ''d'') of the coiled-coil structure.

Our results show that the addition of TFE caused an increase in the α-helical content of the C-terminal region, whereas the head-to-tail affinity decreased. A similar effect is

observed with increasing ionic strength where Tm loses the ability to polymerize, whereas the coiled-coil structure is stabilized (22–26,47). It is thought that the large number of charged residues in the head-to-tail overlap region plays a fundamental role in the ionic-strength dependence of complex formation (6,25,29,47,96,97). Conditions affecting the stability of the Tm coiled-coil structure affect the stability of the head-to-tail complex paradoxically. The association energy between the termini is the difference between the conformational energies of the polypeptides before the interaction and in the complex (29). This and previous studies (29,98) have shown that the association of the Tm termini is accompanied by an increase in the helix content of the C-terminal region. Head-to-tail complex formation could compensate for intramolecular like-charged repulsions (within a coiled-coil dimer) with intermolecular interactions between oppositely charged N- and C-termini (29). The solution structure of the head-to-tail complex (18) indicated that tertiary structures of both N- and C-termini changed upon complex formation, but there was little change in the α-helical content. However, the four C-terminal residues are more disordered in the free C-terminus than in the complex (18). These structural changes may be related to the observed changes in CD spectra (increased helix content) observed upon head-to-tail complex formation in this and other studies (29,98). In conditions of high ionic strength, small counterions in solution can shield negative charges at the C-terminus. This would favor the folding of the chain and as a result disfavor the head-to-tail association since the energy difference (and therefore the gain in stability) would be reduced. TFE may cause a similar effect on the intricate balance between helical stability and head-to-tail complex formation: the helix-inducing character of this solvent that favors the folding of the Tm termini would reduce the energy difference between the dissociated and associated states, thereby disfavoring complex formation. On the other hand, glycerol did not affect head-to-tail association, possibly because its stabilizing effect is related to the packing of already formed coiled-coil regions and does not induce an increase in the helical content of the Tm chains. This could be especially important for the less-structured C-terminal region. The solution NMR structure of the head-to-tail complex (18) demonstrated that the complex is stabilized by hydrophobic contacts involving N-terminal residues M-1, I-4, M-8, L-11, and C-terminal residues L-274, A-277, M-281, and I-284. Most of the ionic interactions in the complex region were intrachain and so it was proposed that ionic interactions could be contributing principally to the stabilization of the structure of the individual chains. Although high concentrations of TFE are known to destabilize tertiary structures (60–62), we showed here that low concentrations of TFE (up to 15%) did not reduce the concentration dependence of the midpoint of the thermal denaturation transition. Indeed, TFE increased the shift in T_m observed by a 15-fold increase in Tm concentration by $\sim$1°C more than that observed in its absence. This result indicates that the concentration of 15% TFE employed does not significantly affect the hydrophobic contacts between the chains.

Based on these results we can attempt to rationalize our observations regarding the conformational stability of the Tm fragments and of the head-to-tail complex. In low ionic strength conditions, the formation of the head-to-tail complex increases the negative ellipticity of the mixture (29). Increasing the ionic strength stabilizes the folded form of the free N- and C-terminal coiled-coils (28) while at the same time destabilizing the complex, probably by shielding charged residues and reducing the electrostatic interactions. In the presence of glycerol, regions already folded in a coiled-coil conformation are stabilized but the overall secondary structure is maintained. Therefore, structural changes which occur during head-to-tail complex formation are also maintained. In the presence of TFE, conformational stability is accompanied by a conformational change that increases helix content of the chains and increases the stability of the uncomplexed coiled-coils. This stabilization could inhibit the separation of the C-terminal strands observed upon complex formation in the solution structure (18). The fact that TFE abolishes instead of stabilizing the head-to-tail complex suggests that it has an effect on the structures of the regions of the Tm fragments involved in the interaction. Apparently however, the TFE-induced structural change is not on the pathway of structural changes that lead to head-to-tail complex formation.

REFERENCES

1. Smillie, L. B. 1979. Structure and functions of tropomyosins from muscle and non-muscle sources. *Trends Biochem. Sci.* 4:151–155.
2. Farah, C. S., and F. C. Reinach. 1995. The troponin complex and regulation of muscle contraction. *FASEB J.* 9:755–767.
3. Squire, J. M., and E. P. Morris. 1998. A new look at thin filament regulation in vertebrate skeletal muscle. *FASEB J.* 12:761–771.
4. Gordon, A. M., E. Homsher, and M. Regnier. 2000. Regulation of contraction in striated muscle. *Physiol. Rev.* 80:853–924.
5. Perry, S. V. 2001. Vertebrate tropomyosin: distribution, properties and function. *J. Muscle Res. Cell Motil.* 22:5–49.
6. McLachlan, A. D., and M. Stewart. 1975. Tropomyosin coiled-coil interactions: evidence for an unstaggered structure. *J. Mol. Biol.* 98: 293–304.
7. McLachlan, A. D., and M. Stewart. 1976. The 14-fold periodicity in alpha-tropomyosin and the interaction with actin. *J. Mol. Biol.* 103: 271–298.
8. Burkhard, P., J. Stetefeld, and S. V. Strelkov. 2001. Coiled coils: a highly versatile protein folding motif. *Trends Cell Biol.* 11:82–88.
9. Lu, S. M., and R. S. Hodges. 2004. Defining the minimum size of a hydrophobic cluster in two-stranded α-helical coiled-coils: effects on protein stability. *Protein Sci.* 13:714–726.
10. Lupas, A. N., and M. Gruber. 2005. The structure of α-helical coiled-coils. *Adv. Protein Chem.* 70:37–38.
11. Phillips, G. N. Jr., E. E. Lattman, P. Cummins, K. Y. Lee, and C. Cohen. 1979. Crystal structure and molecular interactions of tropomyosin. *Nature.* 278:413–417.
12. Ohtsuki, I., K. Maruyama, and S. Ebashi. 1986. Regulatory and cytoskeletal proteins of vertebrate skeletal muscle. *Adv. Protein Chem.* 38: 1–67.

13. Zot, A. S., and J. D. Potter. 1987. Structural aspects of troponin-tropomyosin regulation of skeletal muscle contraction. *Annu. Rev. Biophys. Biophys. Chem.* 16:535–559.

14. Greenfield, N. J., G. T. Montelione, R. S. Farid, and S. E. Hitchcock-DeGregori. 1998. The structure of the N-terminus of striated muscle α-tropomyosin in a chimeric peptide: nuclear magnetic resonance structure and circular dichroism studies. *Biochemistry.* 37:7834–7843.

15. Brown, J. H., K. H. Kim, G. Jun, N. J. Greenfield, R. Dominguez, N. Volkmann, S. E. Hitchcock-Degregori, and C. Cohen. 2001. Deciphering the design of the tropomyosin molecule. *Proc. Natl. Acad. Sci. USA.* 98:8496–8501.

16. Greenfield, N. J., G. V. T. Swapna, Y. Huang, T. Palm, S. Graboski, G. T. Montelione, and S. E. Hitchcock-DeGregori. 2003. The structure of the carboxyl terminus of striated α-tropomyosin in solution reveals an unusual parallel arrangement of interacting α-helices. *Biochemistry.* 42:614–619.

17. Li, Y., S. Mui, J. H. Brown, J. Strand, L. Reshetnikova, L. S. Tobacman, and C. Cohen. 2002. The crystal structure of the C-terminal fragment of striated-muscle α-tropomyosin reveals a key troponin T recognition site. *Proc. Natl. Acad. Sci. USA.* 28:7378–7383.

18. Greenfield, N. J., Y. J. Huang, G. V. T. Swapna, A. Bhattacharya, B. Rapp, A. Singh, G. T. Montelione, and S. E. Hitchcock-DeGregori. 2006. Solution NMR structure of the junction between tropomyosin molecules: implications for actin binding and regulation. *J. Mol. Biol.* 364:80–96.

19. Phillips, G. N. Jr., J. P. Fillers, and C. Cohen. 1986. Tropomyosin crystal structure and muscle regulation. *J. Mol. Biol.* 192:111–131.

20. Palm, T., S. Graboski, S. E. Hitchcock-DeGregori, and N. J. Greenfield. 2001. Disease-causing mutations in cardiac troponin T: identification of a critical tropomyosin-binding region. *Biophys. J.* 81:2827–2837.

21. Greenfield, N. J., T. Palm, and S. E. Hitchcock-DeGregori. 2002. Structure and interactions of the carboxyl terminus of striated muscle α-tropomyosin: it is important to be flexible. *Biophys. J.* 83:2754–2766.

22. Kay, C. M., and K. Bailey. 1960. Light scattering in solutions of native and guanidinated rabbit tropomyosin. *Biochim. Biophys. Acta.* 40: 149–156.

23. Ooi, T., K. Mihashi, and H. Kobayashi. 1962. On polymerization of tropomyosin. *Arch. Biochem. Biophys.* 98:1–11.

24. McCubbin, W. D., and C. M. Kay. 1969. Physicochemical studies on the aggregation of bovine cardiac tropomyosin with ionic strength. *Can. J. Biochem.* 47:411–414.

25. Heeley, D. H., M. H. Watson, A. S. Mak, P. Dubord, and L. B. Smillie. 1989. Effect of phosphorylation on the interaction and functional properties of rabbit striated muscle alpha alpha-tropomyosin. *J. Biol. Chem.* 264:2424–2430.

26. Mo, J. M., M. E. Holtzer, and A. Holtzer. 1990. The thermal denaturation of nonpolymerizable alpha alpha-tropomyosin and its segments as a function of ionic strength. *Biopolymers.* 30:921–927.

27. Heeley, D. H. 1994. Investigation of the effects of phosphorylation of rabbit striated muscle alpha alpha-tropomyosin and rabbit skeletal muscle troponin-T. *Eur. J. Biochem.* 221:129–137.

28. Paulucci, A. A., L. Hicks, A. Machado, M. T. M. Miranda, C. M. Kay, and C. S. Farah. 2002. Specific sequences determine the stability and cooperativity of folding of the C-terminal half of tropomyosin. *J. Biol. Chem.* 277:39574–39584.

29. Paulucci, A. A., A. M. Katsuyama, A. D. Sousa, and C. S. Farah. 2004. A specific C-terminal deletion in tropomyosin results in a stronger head-to-tail interaction and increased polymerization. *Eur. J. Biochem.* 271:589–600.

30. Sönnichsen, F. D., J. E. Van Eyk, R. S. Hodges, and B. D. Sykes. 1992. Effect of trifluoroethanol on protein secondary structure: an NMR and CD study using a synthetic actin peptide. *Biochemistry.* 31: 8790–8798.

31. Slupsky, C. M., C. M. Kay, F. C. Reinach, L. B. Smillie, and B. D. Sykes. 1995. Calcium-induced dimerization of troponin C: mode of interaction and use of trifluoroethanol as a denaturant of quaternary structure. *Biochemistry.* 34:7365–7375.

32. Shiraki, K., K. Nishikawa, and Y. Goto. 1995. Trifluoroethanol-induced stabilization of the α-helical structure of β-lactoglobulin: implication for non-hierarchical protein folding. *J. Mol. Biol.* 245: 180–194.

33. Feinberg, J., F. Heitz, Y. Benyamin, and C. Roustan. 1996. The N-terminal sequence (5–20) of thymosin β4 binds to momeric actin in an α-helical conformation. *Biochem. Biophys. Res. Commun.* 222: 127–132.

34. Kentsis, A., and T. R. Sosnick. 1998. Trifluoroethanol promotes helix formation by destabilizing backbone exposure: desolvation rather than native hydrogen bonding defines the kinetic pathway of dimeric coiled-coil folding. *Biochemistry.* 37:14613–14622.

35. Celinski, S. A., and J. M. Scholtz. 2002. Osmolyte effects on helix formation in peptides and the stability of coiled-coils. *Protein Sci.* 11: 2048–2051.

36. Nelson, J. W., and N. R. Kallenbach. 1986. Stabilization of the ribonuclease S-peptide alpha-helix by trifluoroethanol. *Proteins.* 1:211–217.

37. Jasanoff, A., and A. R. Fersht. 1994. Quantitative determination of helical propensities from trifluoroethanol titration curves. *Biochemistry.* 33:2129–2135.

38. Storrs, R. W., D. Truckess, and D. E. Wemmer. 1992. Helix propagation in trifluoroethanol solutions. *Biopolymers.* 32:1695–1702.

39. Gekko, K., and S. N. Timasheff. 1981. Mechanism of protein stabilization by glycerol: preferential hydration in glycerol-water mixtures. *Biochemistry.* 20:4667–4676.

40. Gekko, K., and S. N. Timasheff. 1981. Thermodynamic and kinetic examination of protein stabilization by glycerol. *Biochemistry.* 20: 4677–4686.

41. Dürr, E., and I. Jelesarov. 2000. Thermodynamic analysis of cavity creating mutations in an engineered leucine zipper and energetics of glycerol-induced coiled-coil stabilization. *Biochemistry.* 39:4472–4482.

42. Meng, F. G., Y. K. Hong, H. W. He, A. E. Lyubarev, B. I. Kurganov, Y. B. Yan, and H. M. Zhou. 2004. Osmophobic effect of glycerol on irreversible thermal denaturation of rabbit creatine kinase. Biophys. J. 87:2247–2254.

43. Haque, I., R. Singh, A. A. Moosavi-Movahedi, and F. Ahmad. 2005. Effect of polyol osmolytes on ΔG_D, the Gibbs energy of stabilization of proteins at different pH values. *Biophys. Chem.* 117:1–12.

44. Zancan, P., and M. Sola-Penna. 2005. Trehalose and glycerol stabilize and renature yeast inorganic pyrophosphatase inactivated by very high temperatures. *Arch. Biochem. Biophys.* 444:52–60.

45. Mishra, R., R. Seckler, and R. Bhat. 2005. Efficient refolding of aggregation-prone citrate synthase by polyol osmolytes: how well protein folding and stability aspects coupled? *J. Biol. Chem.* 280:15553–15560.

46. Tiwari, A., and R. Bhat. 2006. Stabilization of yeast hexokinase A by polyol osmolytes: correlation with the physicochemical properties of aqueous solutions. *Biophys. Chem.* 124:90–99.

47. Sousa, A. D., and C. S. Farah. 2002. Quantitative analysis of tropomyosin linear polymerization equilibrium as a function of ionic strength. *J. Biol. Chem.* 277:2081–2088.

48. Corrêa, F., and C. S. Farah. 2005. Using 5-hydroxytryptophan as a probe to follow protein-protein interactions and protein folding transitions. *Protein Pept. Lett.* 12:241–244.

49. Studier, F. W., A. H. Rosenberg, J. J. Dunn, and J. W. Dubendorff. 1990. Use of T7 RNA polymerase to direct expression of cloned genes. *Methods Enzymol.* 185:60–89.

50. Monteiro, P. B., R. C. Lataro, J. A. Ferro, and F. C. Reinach. 1994. Functional alpha-tropomyosin produced in *Escherichia coli*. A dipeptide extension can substitute the amino-terminal acetyl group. *J. Biol. Chem.* 269:10461–10466.

51. Farah, C. S., and F. C. Reinach. 1999. Regulatory properties of recombinant tropomyosins containing 5-hydroxytryptophan: Ca^{2+}-binding to troponin results in a conformational change in a region of tropomyosin outside the troponin binding site. *Biochemistry.* 38:10543–10551.

52. Hartree, E. F. 1972. Determination of protein: a modification of the Lowry method that gives a linear photometric response. *Anal. Biochem.* 48:422–427.

53. Pace, C. N., and J. M. Scholtz. 1987. Measuring the conformational stability of a protein. *In* Protein Structure: A Practical Approach, 2nd ed. T. E. Creighton, editor. Oxford University Press, New York. 299–321.

54. Mateu, M. G., and A. R. Fersht. 1998. Nine hydrophobic side chains are key determinants of the thermodynamic stability and oligomerization status of tumour suppressor p53 tetramerization domain. *EMBO J.* 17:2748–2758.

55. Lau, S. Y., A. K. Taneja, and R. S. Hodges. 1984. Synthesis of a model protein of defined secondary and quaternary structure. Effect of chain length on the stabilization and formation of two-stranded alpha-helical coiled-coils. *J. Biol. Chem.* 259:13253–13261.

56. Monera, O. D., N. E. Zhou, C. M. Kay, and R. S. Hodges. 1993. Comparison of antiparallel and parallel two-stranded alpha-helical coiled-coils. Design, synthesis, and characterization. *J. Biol. Chem.* 268:19218–19227.

57. Zhou, N. E., C. M. Kay, and R. S. Hodges. 1994. The role of interhelical ionic interactions in controlling protein folding and stability. De novo designed synthetic two-stranded alpha-helical coiled-coils. *J. Mol. Biol.* 237:500–512.

58. Holtzer, M. E., and A. Holtzer. 1995. The use of spectral decomposition via the convex constraint algorithm in interpreting the CD-observed unfolding transitions of coiled coils. *Biopolymers.* 36:365–379.

59. Holtzer, A., M. E. Holtzer, and J. Scolnick. 1989. Does the unfolding transition of two-chain, coiled-coil proteins involve a continuum of intermediates? *In* Protein Folding: Deciphering the Second Half of the Genetic Code. L. M. Gierasch and J. King, editors. American Association for the Advancement of Science, Washington D.C. 177–190.

60. Buck, M., H. Schwalbe, and C. M. Dobson. 1995. Characterization of conformational preferences in a partly folded protein by heteronuclear NMR spectroscopy: assignment and secondary structure analysis of hen egg-white lysozyme in trifluoroethanol. *Biochemistry.* 34:13219–13232.

61. Schonbrunner, N., J. Wey, J. Engels, H. Georg, and T. Kiefhaber. 1996. Native like β-structure in trifluoroethanol-induced partially folded state of the all-β-sheet protein tendamistat. *J. Mol. Biol.* 260:432–445.

62. Shiraki, K., K. Nishikawa, and Y. Goto. 1995. Trifluoroethanol-induced stabilization of the α-helical structure of β-lactoglobulin: implication for non-hierarchical protein folding. *J. Mol. Biol.* 245: 180–194.

63. Holtzer, M. E., A. Holtzer, and J. Skolnick. 1983. α-helix-to-random-coil transition of two-chain, coiled-coils. Theory and experiments for thermal denaturation of α-tropomyosin. *Macromolecules.* 16:173–180.

64. Holtzer, M. E., D. L. Crimmins, and A. Holtzer. 1994. Structural stability of short subsequences of the tropomyosin chain. *Biopolymers.* 35:125–136.

65. Dragan, A. I., and P. L. Privalov. 2002. Unfolding of a leucine zipper is not a simple two-state transition. *J. Mol. Biol.* 321:891–908.

66. MacPhee, C. E., M. A. Perugini, W. H. Sawyer, and G. J. Howlett. 1997. Trifluoroethanol induces the self-association of specific amphipathic peptides. *FEBS Lett.* 416:265–268.

67. Maroun, R. G., D. Krebs, S. El Antri, A. Deroussent, E. Lescot, F. Troalen, H. Porumb, M. E. Goldberg, and S. Fermandjian. 1999. Self-association and domains of interactions of an amphipathic helix peptide inhibitor of HIV-1 integrase assessed by analytical ultracentrifugation and NMR experiments in trifluoroethanol/H(2)O mixtures. *J. Biol. Chem.* 274:34174–34185.

68. Asghari, S. M., K. Khajeh, B. Ranjbar, R. H. Sajedi, and H. Naderi-Manesh. 2004. Comparative studies on trifluoroethanol (TFE) state of a thermophilic α-amylase and its mesophilic counterpart: limited proteolysis, conformational analysis, aggregation and reactivation of the enzymes. *Int. J. Biol. Macromol.* 34:173–179.

69. Pace, C. N., D. V. Laurents, and J. A. Thomson. 1990. pH dependence of the urea and guanidine hydrochloride denaturation of ribonuclease A and ribonuclease T1. *Biochemistry.* 29:2564–2572.

70. Myers, J. K., C. N. Pace, and J. M. Scholtz. 1995. Denaturant m values and heat capacity changes: relation to changes in accessible surface areas of protein unfolding. *Protein Sci.* 4:2138–2148.

71. Shortle, D. 1995. Staphylococcal nuclease: a showcase of m-value effects. *Adv. Protein Chem.* 46:217–247.

72. Chiti, F., N. Taddei, P. Webster, D. Hamada, T. Fiaschi, G. Ramponi, and C. M. Dobson. 1999. Acceleration of the folding of acylphosphatase by stabilization of local secondary structure. *Nat. Struct. Biol.* 6: 380–387.

73. Main, E. R. G., and S. E. Jackson. 1999. Does trifluoroethanol affect folding pathways and can it be used as a probe of structure in transition states? *Nat. Struct. Biol.* 6:831–835.

74. Timasheff, S. N. 1993. The control of protein stability and association by weak interactions with water: how do solvents affect these processes? *Annu. Rev. Biophys. Biomol. Struct.* 22:67–97.

75. Mak, A. S., and L. Smillie. 1981. Non-polymerizable tropomyosin: preparation, some properties and F-actin binding. *Biochem. Biophys. Res. Commun.* 101:208–214.

76. Dabrowska, R., E. Nowak, and W. Drabikowski. 1983. Some functional properties of nonpolymerizable and polymerizable tropomyosin. *J. Muscle Res. Cell. Motil.* 4:143–161.

77. Moraczewska, J., and S. E. Hitchcock-DeGregori. 2000. Independent functions for the N- and C-termini in the overlap region of tropomyosin. *Biochemistry.* 39:6891–6897.

78. Pato, M. D., A. S. Mak, and L. B. Smillie. 1981. Fragments of rabbit striated muscle alpha-tropomyosin. II. Binding to troponin-T. *J. Biol. Chem.* 256:602–607.

79. Heeley, D. H., K. Golosinska, and L. B. Smillie. 1987. The effects of troponin T fragments T1 and T2 on the binding of nonpolymerizable tropomyosin to F-actin in the presence and absence of troponin I and troponin C. *J. Biol. Chem.* 262:9971–9978.

80. Hitchcock-DeGregori, S. E., and R. W. Heald. 1987. Altered actin and troponin binding of amino-terminal variants of chicken striated muscle α-tropomyosin expressed in *Escherichia coli*. *J. Biol. Chem.* 262: 9730–9735.

81. Heald, R. W., and S. E. Hitchcock-DeGregori. 1988. The structure of the amino terminus of tropomyosin is critical for binding to actin in the absence and presence of troponin. *J. Biol. Chem.* 263:5254–5259.

82. Cho, Y.-J., J. Liu, and S. E. Hitchcock-DeGregori. 1990. The amino terminus of muscle tropomyosin is a major determinant for function. *J. Biol. Chem.* 265:538–545.

83. Willadsen, K. A., C. A. Butters, L. E. Hill, and L. S. Tobacman. 1992. Effects of the amino-terminal regions of tropomyosin and troponin T on thin filament assembly. *J. Biol. Chem.* 267:23746–23752.

84. Butters, C. A., K. A. Willadsen, and L. S. Tobacman. 1993. Cooperative interactions between adjacent troponin-tropomyosin complexes may be transmitted through the actin filament. *J. Biol. Chem.* 268: 15565–15570.

85. Hill, L. E., J. P. Mehegan, C. A. Butters, and L. S. Tobacman. 1992. Analysis of troponin-tropomyosin binding to actin. Troponin does not promote interactions between tropomyosin molecules. *J. Biol. Chem.* 267:16106–16113.

86. Moraczewska, J., K. Nicholson-Flynn, and S. E. Hitchcock-DeGregori. 1999. The ends of tropomyosin are major determinants of actin affinity and myosin subfragment-1 induced binding to F-actin in the open state. *Biochemistry.* 38:15885–15892.

87. Moraczewska, J. 2002. Structural determinants of cooperativity in actomyosin interactions. *Acta Biochim. Pol.* 49:805–812.

88. Mckillop, D. F., and M. A. Geeves. 1993. Regulation of the interaction between actin and myosin subfragment 1: evidence for three states of the thin filament. *Biophys. J.* 65:693–701.

89. Phillips, G. N. Jr., and S. Chako. 1996. Mechanical properties of tropomyosin and implications for muscle regulation. *Biopolymers.* 38:89–95.

90. Bacchiocchi, C., and S. S. Lehrer. 2002. Ca2+ induced movement of tropomyosin in skeletal muscle thin filaments observed by multi-site FRET. *Biophys. J.* 82:1524–1536.

91. Holthauzen, L. M., F. Corrêa, and C. S. Farah. 2004. Ca^{2+}-induced rolling of tropomyosin in muscle thin filaments: the alpha- and beta-band hypothesis revisited. *J. Biol. Chem.* 279:15204–15213.

92. Singh, A., and S. E. Hitchcock-DeGregori. 2003. Local destabilization of the tropomyosin coiled-coil gives the molecular flexibility required for actin binding. *Biochemistry.* 42:14114–14121.

93. Singh, A., and S. E. Hitchcock-DeGregori. 2006. Dual requirement for flexibility and specificity for binding of the coiled-coil tropomyosin to its target, actin. *Structure.* 14:43–50.

94. Pato, M. D., and L. B. Smillie. 1978. Stability and troponin-T binding properties of rabbit skeletal alpha-tropomyosin fragments. *FEBS Lett.* 87:95–98.

95. Holtzer, M. E., and A. Holtzer. 1990. Alpha-helix to random coil transitions of two-chain coiled coils: experiments on the thermal denaturation of isolated segments of alpha alpha-tropomyosin. *Biopolymers.* 30:985–993.

96. Johnson, P., and L. B. Smillie. 1977. Polymerizability of rabbit skeletal tropomyosin: effects of enzymatic and chemical modifications. *Biochemistry.* 16:2264–2269.

97. Mak, A., L. B. Smillie, and M. Barany. 1978. Specific phosphorylation at serine-283 of alpha tropomyosin from frog skeletal and rabbit skeletal and cardiac muscle. *Proc. Natl. Acad. Sci. USA.* 75:3588–3592.

98. Palm, T., N. J. Greenfield, and S. E. Hitchcock-DeGregori. 2003. Tropomyosin ends determine the stability and functionality of overlap and troponin T complexes. *Biophys. J.* 84:3181–3189.